

Strange nonchaotic attractors in driven excitable systems

Awadhesh Prasad,¹ Bibudhananda Biswal,^{2,3} and Ramakrishna Ramaswamy⁴

¹*Department of Bioengineering, Arizona State University, Tempe, Arizona 85287, USA*

²*Sri Venkateswara College, Delhi University, New Delhi 110 021 India*

³*ICAI, University of Stuttgart, Pfaffenwaldring 27, D-70569 Stuttgart, Germany*

⁴*School of Physical Sciences, Jawaharlal Nehru University, New Delhi 110 067, India*

(Received 26 March 2003; published 18 September 2003)

Through quasiperiodic forcing, an excitable system can be driven into a regime of spiking behavior that is both aperiodic and stable. This is a consequence of strange nonchaotic dynamics: the motion of the system is on a fractal attractor and the largest Lyapunov exponent is negative.

DOI: 10.1103/PhysRevE.68.037201

PACS number(s): 05.45.-a

Many physical and physiological systems [1,2] show spontaneous spiking behavior. These are *excitable* dynamical systems [3]: for external perturbation below a threshold the dynamics remains in a quiescent state, whereas drastically different dynamics results for perturbation above the threshold. Excitability has been observed in numerous fields, e.g., chemical reaction kinetics, solid state physics, biology, etc. [4]. The well-known neuronal Fitzhugh-Nagumo system [5] has been studied extensively in this context. Irregular intensity dropouts in feedback lasers have also been modeled as an excitable system [6]. Under the effect of external noise such systems have dynamics with an aperiodic sequence of spikes. There can be stochastic or coherence resonance [7] as well.

The simplest models showing excitable dynamics are forced systems with two spatial freedoms [3] so that in the absence of perturbation the dynamics is entirely periodic or quasiperiodic. It is also necessary that there be a saddle as well as other fixed points so that the system can be driven from the vicinity of one node to another by the dynamics [3]. In systems that have been studied so far, both periodic driving as well as noise have been used to cause perturbations [8–10].

Here we examine the effect of quasiperiodic forcing in excitable systems. The motivation for this study comes from the experience that in numerous other dynamical systems the effect of quasiperiodic driving is to create attractors that are both stable and fractal [11]. Quasiperiodicity is in some sense intermediate in effect between purely periodic driving and noise, and generically appears to create strange nonchaotic attractors (SNAs). We are therefore interested in the nature of the attractors and excitable dynamics under quasiperiodic driving in the present work.

Our first application is made on a system introduced by Eguia, Mindlin, and Giudici [6] that models low-frequency fluctuations in a semiconductor laser with optical feedback,

$$\begin{aligned} \dot{x} &= y, \\ \dot{y} &= x - y - x^3 + xy + \epsilon_1 + \epsilon_2 x^2. \end{aligned} \quad (1)$$

This set of equations, when driven by noise, has been shown to simulate the observed irregular pattern of intensity fluctuations reasonably well, and a statistical description of

the dropouts has also been discussed [3]. The phase diagram for the unforced system in the ϵ_1 - ϵ_2 plane [1] has four separate regions based on the number and type of fixed points. In one such region a saddle coexists with a stable node, and Fig. 1 shows the phase curves. The unstable manifold (solid line) of the saddle (\star) terminates in a stable node (\bullet), while the stable manifold of the saddle (the dashed line) connects to the coexisting unstable focus (\circ). Since the only attractor is the stable node, any trajectory that is made to cross the stable manifold of the saddle by a perturbation necessarily makes a long excursion to reach the attractor. This dynamical behavior, which is independent of the strength of the perturbation so long as it is above the threshold, makes this system excitable.

Forcing is introduced into this system through time dependence in the control parameter:

$$\epsilon_1 \rightarrow F(t)\epsilon_1, \quad (2)$$

where the modulation $F(t) = 1 + \epsilon(\cos t + \cos \omega t)$ will be quasiperiodic in time if ω is chosen to be an irrational number. We take this frequency to be the inverse golden-mean ratio $(\sqrt{5}-1)/2$.

Compared to the periodic or noise driven case [3], quasiperiodic forcing drastically alters the characteristic behavior

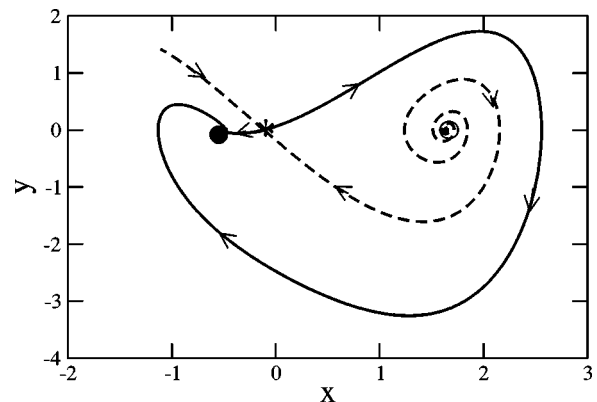


FIG. 1. Phase curves in the excitable region at $\epsilon_1 = 0.08$ and $\epsilon_2 = 1$ in Eq. (1). The symbols \star , \circ , and \bullet represent the saddle, unstable focus, and stable node, respectively, as discussed in the text.

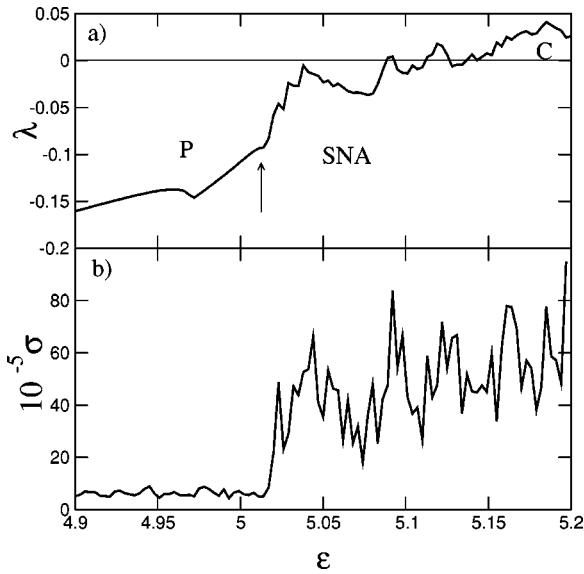


FIG. 2. (a) The largest Lyapunov exponent and (b) its variance as a function of ϵ . P and C indicate the periodic and chaotic regimes, respectively.

of the spiking. Complex attractors that are geometrically strange can be created, and on these the dynamics can become chaotic or remain nonchaotic, depending on the magnitude of ϵ . We present detailed numerical results [12] for representative values of the parameters, here taken to be $\epsilon_1 = 0.08$ and $\epsilon_2 = 1$. In Fig. 2(a) the largest Lyapunov exponent (LE) is plotted as a function of ϵ . In order to detect the occurrence of complex dynamical behavior, we also examine the variance of a set of finite-time estimates of the Lyapunov exponent, shown in Fig. 2(b). A significant increase in the fluctuations is observed at a sharp transition value of $\epsilon \sim 5.02$ even though the LE remains negative. This is characteristic of SNAs [13]. Shown in Fig. 3(a) is the limit cycle for the system at $\epsilon = 5$ with the unstable node indicated by \bullet . Under quasiperiodic forcing, this limit cycle transforms into a fractal attractor (at a transition value of $\epsilon \approx 5.02$). This attractor is shown in Fig. 3(b) at $\epsilon = 5.08$, slightly above the transition. The Lyapunov exponent being negative, the dynamics remain stable: the synchronization of two trajectories with very different initial conditions is shown in Fig. 3(c). This is a very robust property of strange nonchaotic attractors [14].

The transition from a limit cycle attractor to a SNA is detected using the observation that, although the largest LE remains negative, its variance (obtained, say from a sample of finite-time Lyapunov exponents) shows an abrupt and sharp increase [see Figs. 2(a) and 2(b)]. This coincides with a crisislike behavior [15], i.e., a sudden expansion of the attractor. In this case this increase in the volume of the attractor occurs through a sharp transition from a limit cycle to a fractal attractor. As in all SNAs, the motion is intermittent [13,16,17] and nearby trajectories with different initial conditions synchronize in time [Fig. 3(c)].

Because of the combination of intermittency and excitability, the present system does, however, exhibit an important difference from other SNAs that have been studied ear-

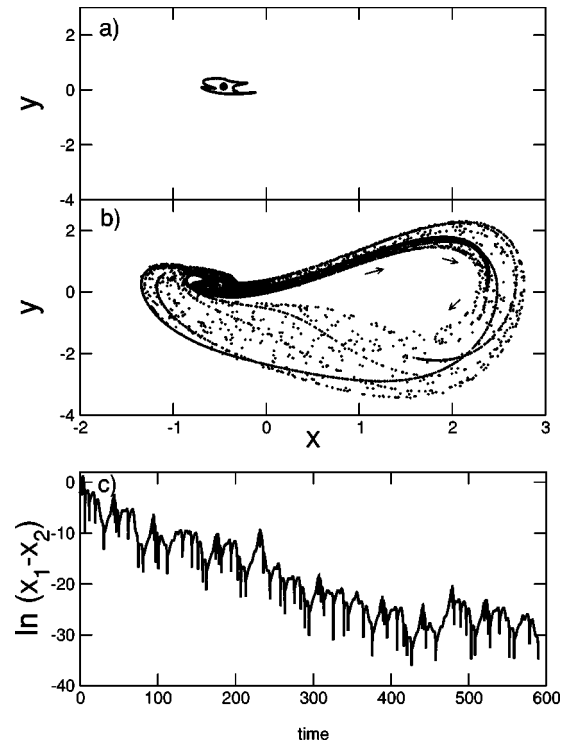


FIG. 3. The Poincaré section in the phase plane at (a) $\epsilon = 5$ (periodic attractor) (\bullet is the stable node for the unforced case, $\epsilon = 0$) and (b) $\epsilon = 5.08$ (SNA), and (c) the difference between the signals of two uncoupled identical systems Eq. (1), with different initial conditions, showing synchronization.

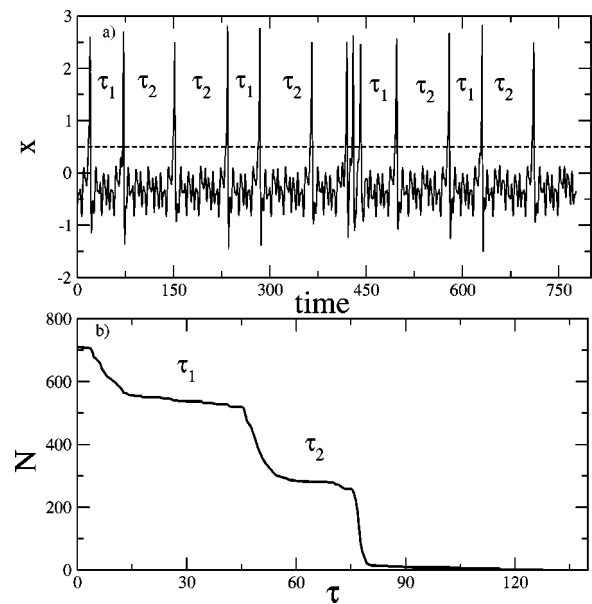


FIG. 4. (a) The variation of x with time. τ_1 and τ_2 are two characteristic time durations in which the trajectory remains close to the periodic attractor. (b) The distribution $N(\tau)$ of durations τ on the SNA with $\epsilon = 5.081$. The interspike intervals are measured by threshold crossings [see the dashed line in (a)].

lier. Excitable SNAs have an unusual distribution of interspike intervals. The variation of x , plotted in Fig. 4(a), shows these characteristic bursts or spikes. In the interspike region the trajectory remains near the fixed point of the unperturbed system while spiking takes the system along the main part of the attractor. The interspike intervals $\{\tau\}$ have the characteristic distribution shown in Fig. 4(b). $N(\tau)$ is the number of intervals of duration $\geq \tau$. Two distinct scaling regimes are evident, in contrast to other examples of intermittent SNAs [16,18] or chaotic attractors in other nonexcitable systems [19].

The mechanism for the interspike plateaus shown in Fig. 4(b) is the following. The two time scales originate from the two different circuits on the attractor. The system stays mostly in the vicinity of the fixed point or on the limit cycle. This is the low-amplitude fluctuations in Fig. 4(a). The bursts or spikes occur when the trajectory goes onto the fractal attractor. The long interspike interval τ_2 occurs when the motion goes from the vicinity of the fixed point to the fractal attractor and the short interspike interval τ_1 occurs when the motion on the fractal attractor originates from the limit cycle.

This behavior appears to be a common feature of other quasiperiodically driven excitable systems as well. We extend our study to the van der Pol–Fitzhugh–Nagumo equations [5,7] which model excitable neuronal dynamics. This is also a system with two freedoms, which in reduced form is given by

$$\begin{aligned} \mu \dot{x} &= x - \frac{x^3}{3} - y, \\ \dot{y} &= x + \alpha. \end{aligned} \quad (3)$$

The fast variable x corresponds to the membrane potential and the slow variable y is related to recovery or refractoriness. This system has a fixed point at $(x,y) = (-\alpha, -\alpha + \alpha^3/3)$. For $\alpha < 1$, there is a well-defined natural frequency since the dynamics is oscillatory, while for $\alpha > 1$ the dynamics is stable, although any finite perturbation will produce a large pulse. Thus the system satisfies the criteria of excitability. In Fig. 5(a) the variation of the Lyapunov exponent with parameter ϵ is shown for the modulated system with parameters $\alpha = 1.05$, $\mu = 0.01$,

$$\begin{aligned} \mu \dot{x} &= x - \frac{x^3}{3} - y, \\ \dot{y} &= x + F(\theta)\alpha, \\ \dot{\theta} &= 1. \end{aligned} \quad (4)$$

[The variable θ plays the role of time; trivially, the last of the equations integrates to $\theta = t$. In Fig. 6(c) we consider the variable θ modulo 2π .]

The sudden increase in fluctuations in the finite-time Lyapunov exponent above $\epsilon \sim 0.039$ clearly signifies a transition in the dynamics, which we confirm as being from periodic motion [Fig. 6(a)] to a SNA [Fig. 6(b)]. The strangeness of the SNA can be clearly observed in Fig. 6(c) where

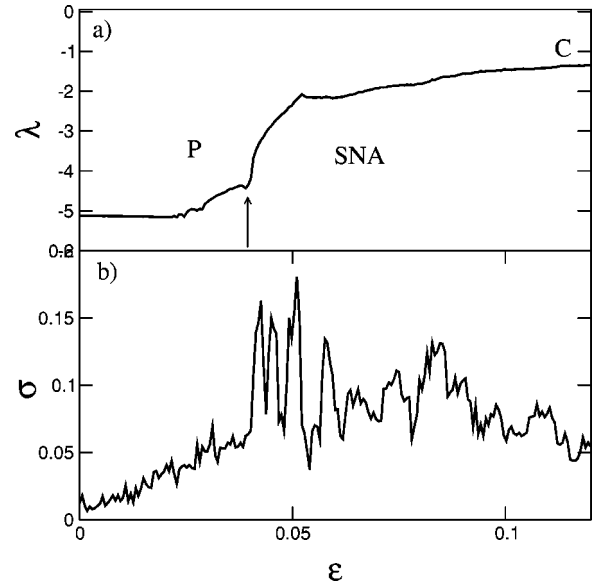


FIG. 5. The (a) largest Lyapunov exponent and (b) variance as a function of ϵ in the Fitzhugh-Nagumo model, Eq. (4).

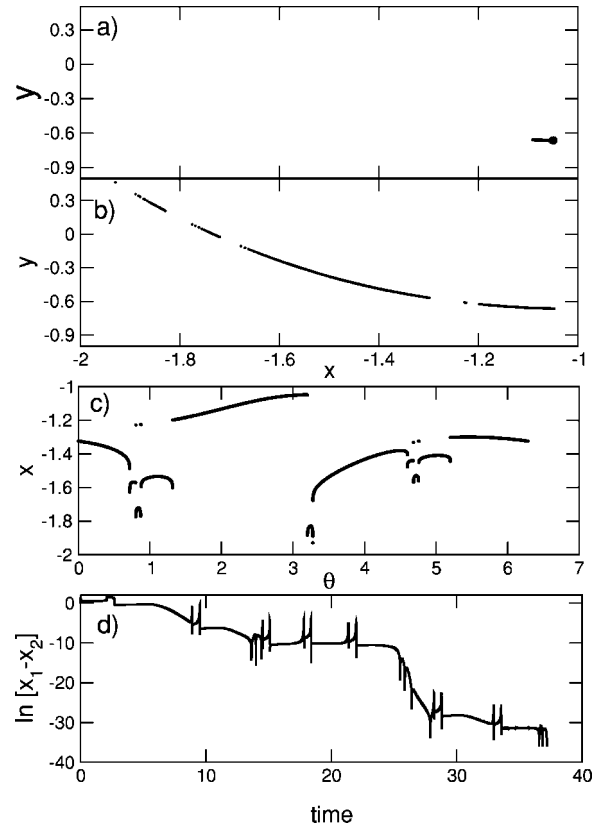


FIG. 6. The Poincaré section in the phase plane at (a) $\epsilon = 0.02$ (periodic attractor) (● is the stable node for unforced case, $\epsilon = 0$) and (b) $\epsilon = 0.1$ (SNA); (c) the $x-\theta$ phase portrait of a typical trajectory, showing the discontinuities on the SNA; and (d) the difference between the signals of two uncoupled identical systems Eq. (4), with different initial conditions, showing synchronization on the SNA.

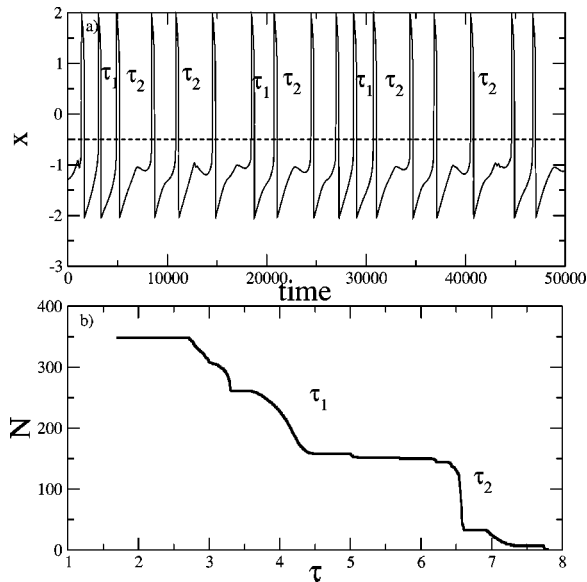


FIG. 7. (a) The variation of x with time and (b) the distribution $N(\tau)$ on the SNA at $\epsilon=0.1$. The interspike intervals are measured by threshold crossings [see the dashed line in (a)].

discontinuities in (θ, x) are shown. The variation of x and the distribution $N(\tau)$ of interspike intervals is shown in Figs. 7(a) and (b), respectively. The general behavior, including synchronization, closely resembles that of the laser system, Eq. (1). The value of ϵ at which the system makes the transition from periodic motion to SNA depends on the value of α , and we observe empirically that SNAs are present over a wide range of parameter ϵ .

All forced excitable systems show spiking phenomena, although as pointed out above the histogram of interspike intervals on the excitable SNA has a characteristic bimodal distribution. Such distributions and return maps constructed from time series data for τ have been extensively used in the analysis of spike data from experimental signals [such as electroencephalograms (EEGs)]. In this context, it was proposed earlier by Mandell and Selz [20], who analyzed EEG data for signatures of SNAs, that quasiperiodic forcing may be a relevant internal mechanism for neuronal dynamics. Although the analysis of a spectral distribution function for SNAs [21] was not conclusive, there was some evidence for a fractal attractor with zero Lyapunov exponent.

In summary, we have shown here that with quasiperiodic driving the simple attractors of excitable systems become geometrically strange and dynamically nonchaotic. In contrast to previously studied systems [13], SNAs do not emerge in the transition from periodic to chaotic dynamics: in the absence of driving, the dynamics is nonchaotic. The present scenario can therefore find application where the contrasting features of aperiodic bursting as well as dynamical stability are simultaneously necessary.

ACKNOWLEDGMENTS

This research was supported by grants from the Department of Science and Technology, India to R.R., and the University Grants Commission, India to B.B. A.P. would like to acknowledge partial funding from the AFOSR and the National Institutes of Health, USA, and Leon Iassemidis for discussions.

-
- [1] A. M. Yacomotti, M. C. Eguia, J. Aliaga, O. E. Martinez, G. B. Mindlin, and A. Lipsich, *Phys. Rev. Lett.* **83**, 292 (1999).
 - [2] F. C. Hoppensteadt and E. M. Izhikevich, *Weakly Connected Neural Networks* (Springer-Verlag, Berlin, 1997).
 - [3] A. C. Ventura, G. B. Mindlin, and S. Ponce Dawson, *Phys. Rev. E* **65**, 046231 (2002).
 - [4] M. C. Cross and P. C. Hohenberg, *Rev. Mod. Phys.* **65**, 851 (1993).
 - [5] R. Fitzhugh, *Biophys. J.* **1**, 455 (1961); B. van der Pol, *Philos. Mag.* **3**, 65 (1927).
 - [6] M. C. Eguia, G. B. Mindlin, and M. Giudici, *Phys. Rev. E* **58**, 2636 (1998).
 - [7] A. S. Pikovsky and J. Kurths, *Phys. Rev. Lett.* **78**, 775 (1997); R. Benzi *et al.*, *J. Phys. A* **14**, L453 (1981).
 - [8] A. Venkatesan and M. Lakshmanan, *Phys. Rev. E* **58**, 3008 (1998).
 - [9] A. Longtin, *J. Stat. Phys.* **70**, 309 (1993).
 - [10] D. T. Kaplan *et al.*, *Phys. Rev. Lett.* **76**, 4074 (1996).
 - [11] C. Grebogi, E. Ott, S. Pelikan, and J. A. Yorke, *Physica D* **13**, 261 (1984).
 - [12] The equations are integrated numerically using a fourth-order Runge-Kutta scheme with step size $2\pi/\omega N$, where N is equal to 100 and 2000 for Eqs. (1) and (4), respectively. Lyapunov exponents and their fluctuations are estimated from a set of finite-time realizations of $n=10^5$ steps.
 - [13] A. Prasad, S. S. Negi, and R. Ramaswamy, *Int. J. Bifurcation Chaos Appl. Sci. Eng.* **11**, 291 (2001), and references therein.
 - [14] R. Ramaswamy, *Phys. Rev. E* **56**, 7294 (1997).
 - [15] C. Grebogi, E. Ott, and J. Yorke, *Phys. Rev. Lett.* **48**, 1507 (1982).
 - [16] A. Prasad, V. Mehra, and R. Ramaswamy, *Phys. Rev. Lett.* **79**, 4127 (1997); *Phys. Rev. E* **57**, 1576 (1998).
 - [17] J. Heagy and W. Ditto, *J. Nonlinear Sci.* **1**, 423 (1991).
 - [18] A. Venkatesan, M. Lakshmanan, A. Prasad, and R. Ramaswamy, *Phys. Rev. E* **61**, 3641 (2000); A. Venkatesan, K. Murali, and M. Lakshmanan, *Phys. Lett. A* **259**, 246 (1999).
 - [19] M. Dubois, M. A. Rubio, and P. Berge, *Phys. Rev. Lett.* **51**, 1446 (1983); A. Prasad and R. Ramaswamy, *Phys. Rev. E* **60**, 2761 (1999).
 - [20] A. J. Mandell and A. Selz, *J. Stat. Phys.* **70**, 355 (1993).
 - [21] W. L. Ditto *et al.*, *Phys. Rev. Lett.* **65**, 533 (1990).